

## Quadrupole Oscillation of a Single-Vortex Bose-Einstein Condensate: Evidence for Kelvin Modes

V. Bretin, P. Rosenbusch, F. Chevy, G.V. Shlyapnikov,\* and J. Dalibard

*Laboratoire Kastler Brossel,† 24 rue Lhomond, 75005 Paris, France*

(Received 5 November 2002; published 12 March 2003)

We study the two transverse quadrupole modes of a cigar-shaped Bose-Einstein condensate with a single centered vortex. We show that the counterrotating mode is more strongly damped than in the absence of a vortex, whereas the corotating mode is not affected appreciably by the vortex. We interpret this result as a decay of the counterrotating quadrupole mode into two excitations of the vortex line, the so-called Kelvin modes. This is supported by direct observation of the vortex line.

DOI: 10.1103/PhysRevLett.90.100403

PACS numbers: 03.75.Lm, 32.80.Pj, 67.40.Vs

When a superfluid described by a macroscopic wave function  $\psi(\mathbf{r})$  is set into rotation, quantized vortex lines appear, along which the density  $|\psi|^2$  is zero [1–3]. Since  $\psi$  is single valued, its phase variation on a closed contour around a vortex line is  $2n\pi$  ( $n$  is an integer). Such vortices have been observed in many systems, e.g., superconductors [4], superfluid liquid helium [5], and gaseous Bose-Einstein condensates [6–9].

A vortex line is a dynamic object. As for a classical string, transverse vibration modes of the line can be excited. For a classical vortex, the modes were calculated by Kelvin in 1880 [10]. His result can be transposed to a single quasilinear quantum vortex with unit charge ( $n = 1$ ) in a homogeneous superfluid. This gives the relation between the energy  $\hbar\omega_K$  of a quantum of the Kelvin modes (kelvon) and its wave vector  $k$  [3,11,12]:

$$\hbar\omega_K \simeq \frac{\hbar^2 k^2}{2m} \ln(1/k\xi) \quad (k\xi \ll 1). \quad (1)$$

Here  $m$  is the mass of a particle of the fluid and  $\xi = (8\pi\rho a)^{-1/2}$  is the healing length ( $a$  is the scattering length characterizing the binary interactions in the fluid and  $\rho$  is the fluid density). Because of the Kelvin-Helmoltz theorem [13], the Kelvin modes rotate always in the sense opposite to the vortex velocity field [3,10]. Consequently, the angular momentum of a kelvon associated with a  $n = 1$  vortex is  $-\hbar$  [14].

The Kelvin modes play an important role in the dynamics of superfluids [5,15] or neutron stars [14]. In superfluid liquid helium  $^4\text{He}$ , they have been observed by trapping ions in the vortex core and exciting them by a circularly polarized electromagnetic field [16].

In this Letter, we present experimental evidence for Kelvin modes excited through nonlinear (Beliaev) decay of the quadrupole mode  $m = -2$ . An elementary excitation of the quadrupole mode  $m = -2$  decays into a pair of kelvons with wave vectors  $k$  and  $-k$ . We measure the corresponding increase of the decay rate with respect to the decay of the  $m = +2$  mode, for which angular momentum conservation forbids such a mechanism. We also present pictures of the rotating condensate obtained after

the excitation of the  $m = -2$  mode. They show a density modulation close to the vortex line. The spatial period of the modulation is in good agreement with the one deduced from the generalization of Eq. (1) to a trapped condensate [17,18] and the energy conservation  $\omega_{-2} = 2\omega_K$  ( $\omega_{-2}$  is the frequency of the  $m = -2$  quadrupole mode).

We use a cigar-shaped  $^{87}\text{Rb}$  condensate held in an axisymmetric Ioffe-Pritchard magnetic trap. The atoms are spin-polarized in the  $F = m_F = 2$  state. The trapping frequencies are  $\omega_z/2\pi = 11.8$  Hz (longitudinal axis) and  $\omega_\perp/2\pi = 98.5$  Hz (transverse plane). The temperature is  $\sim 70$  nK, corresponding to a 70% condensed fraction. The number of atoms in the condensate is  $1.3 \times 10^5$  and the chemical potential is 40 nK.

In order to produce in a reliable way a single vortex centered on the  $z$  axis [19], we follow the procedure outlined in Ref. [20]. We use an off-resonant laser beam, whose motion is controlled by acousto-optic modulators, to superimpose a rotating dipole potential onto the magnetic potential. This dipole potential is asymmetric in the  $x$ - $y$  plane and reads  $m\omega_\perp^2 \epsilon(X^2 - Y^2)/2$  with  $\epsilon = 0.07$ . The axes  $X, Y$  are deduced from the fixed axes  $x, y$  by a rotation of an angle  $\Omega t$ . The dipole potential is switched on after the condensate formation for a period of 0.3 s. We choose  $\Omega$  close to the rotating quadrupole resonance  $\omega_\perp/\sqrt{2}$ , thus creating a lattice with five to seven vortices. During the next 2 sec, the laser stirrer is blocked and the vortex lattice decays due to a slight ( $\sim 1\%$ ) static anisotropy of the magnetic potential in the  $x$ - $y$  plane. The condensate is then left with a single centered vortex. The lifetime of this last vortex is  $\sim 7$  sec, which is much longer than the rest of the experimental sequence. Experiments without vortices performed for comparison follow the same procedure, except that rotation is kept at a lower frequency to prevent any nucleation of vortices.

The dipole potential is then used again on the single vortex condensate to selectively excite the modes  $m = +2$ ,  $m = -2$  or their superposition. During this excitation, the angular frequency and deformation parameter of the dipole potential are set to  $\Omega'$  and  $\epsilon'$ . The duration of the excitation is denoted by  $\tau$ . The state of the condensate

is finally probed after a 25 ms time of flight by simultaneous absorption imaging along the two directions  $y$  and  $z$ . Transverse images (imaging beam along  $y$ ) give indications on the behavior of the vortex line. Quantitative information is obtained from the longitudinal images (imaging beam along  $z$ ). These are fitted assuming an elliptic Thomas-Fermi profile for the spatial density of the condensate in the  $x$ - $y$  plane. We measure the size  $R_l$  and the polar angle  $\theta$  of the long axis, and the size  $R_s$  of the short axis.  $\zeta = R_l/R_s$  denotes the ellipticity in the  $x$ - $y$  plane.

The first series of experiments aims at observing the free evolution of the two quadrupole surface modes  $m = \pm 2$ , in the presence and absence of a vortex. A percussional excitation is performed using the laser stirrer with fixed axes ( $\Omega' = 0$ ) for a short duration  $\tau = 0.5$  ms  $\ll \omega_{\perp}^{-1}$  ( $\epsilon' \sim 1$ ). This excites a superposition of  $m = +2$  and  $m = -2$  modes with equal amplitudes. We then let the cloud evolve freely in the magnetic trap for a variable time  $t$  and we perform the time of flight analysis. The quantities  $\theta$  and  $\zeta$  are plotted as a function of  $t$  in Fig. 1.

In the case where the condensate is vortex-free [Fig. 1(a)], the angle  $\theta$  jumps periodically between 0 and  $\pi/2$ , indicating that the amplitudes of the two quadrupole modes  $m = +2$  and  $m = -2$  stay equal. The situation is dramatically different in the presence of a vortex

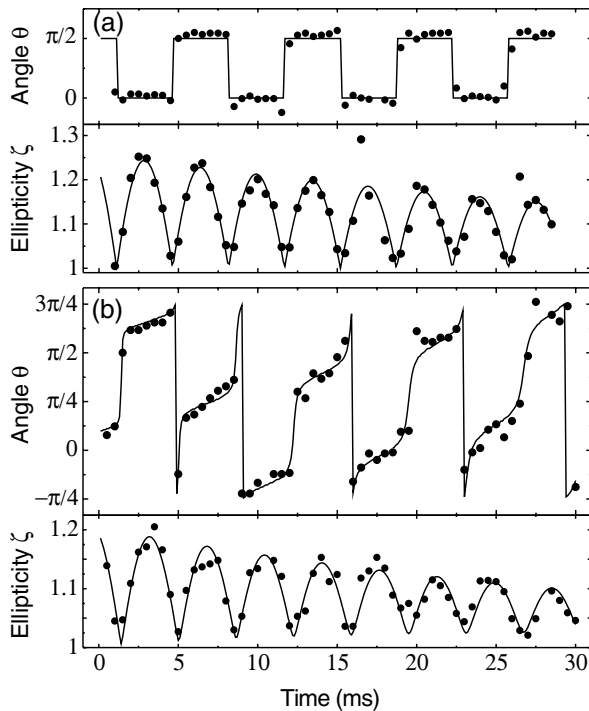


FIG. 1. Angle  $\theta$  and ellipticity  $\zeta$  as a function of  $t$  in the absence (a) and in the presence of a single centered vortex (b). In (b) the precession of the main axes observed for small  $t$  increases at longer times, and the jumps in  $\theta$  become rounded indicating that the mode  $m = -2$  decays faster than the mode  $m = +2$ . The solid lines are fits using the solutions of Eq. (2).

[Fig. 1(b)]. In this case two successive regimes occur: for short times, one still observes the quadrupole oscillation, now with precessing axes. The precession is due to the lift of degeneracy between the frequencies  $\omega_{\pm 2}$  of the two modes  $m = \pm 2$  with  $\omega_{+2} > \omega_{-2}$  [21–24]. This well known effect is often used to measure the angular momentum of the condensate [25–27]. For  $t > 5$  ms, the precession rate increases and the jumps of  $\pi/2$  in  $\theta$  become more and more rounded. This behavior indicates that the mode  $m = -2$  decays faster than  $m = +2$ , which will eventually lead to an atom cloud with nonoscillating ellipticity and constant rotation at  $\omega_{+2}$ .

For a quantitative analysis, we have fitted  $\theta(t)$  and  $\zeta(t)$  assuming that the amplitudes  $\alpha_m$  of the modes  $m = \pm 2$  vary as

$$\dot{\alpha}_m + (i\omega_m + \Gamma_m) \alpha_m = 0 \quad (2)$$

with  $\alpha_{+2}(0) = \alpha_{-2}(0)$ . The decay of the quadrupole modes is modeled using phenomenological linear damping rates  $\Gamma_m$ . A more refined treatment should take into account the nonlinear character of the Beliaev-type process under investigation.

In the case of no vortex [Fig. 1(a)], where the symmetry between the modes  $m = \pm 2$  is preserved, we deduce from the fit  $\omega_{\pm 2}^{(0)}/2\pi = 142.0 \pm 0.5$  Hz, which is close to the prediction in the Thomas-Fermi regime  $\sqrt{2}\omega_{\perp}/2\pi = 139.3$  Hz [28]. For the decay rate we find  $\Gamma_{\pm 2}^{(0)} = 21.3 \pm 1.3$  s $^{-1}$ . In the presence of a vortex [Fig. 1(b)], the fit gives  $\omega_{+2}/2\pi = 159.5 \pm 1.0$  Hz,  $\omega_{-2}/2\pi = 116.8 \pm 1.0$  Hz,  $\Gamma_{+2} = 19.1 \pm 2.0$  s $^{-1}$ , and  $\Gamma_{-2} = 35.7 \pm 4.0$  s $^{-1}$ . We note that the two measured frequencies satisfy the sum rule  $\omega_{+2}^2 + \omega_{-2}^2 = 4\omega_{\perp}^2$  [24] with a good accuracy. The fit confirms the difference in the two decay rates with the addition that the mode  $m = -2$  decays faster in the presence of a vortex ( $\Gamma_{-2} > \Gamma_{+2}^{(0)}$ ), whereas  $\Gamma_{+2} \simeq \Gamma_{\pm 2}^{(0)}$  [29].

In a second series of experiments, we excite the two modes  $m = +2$  and  $m = -2$  separately by a near resonant drive. For the excitation, we set  $\epsilon' = 0.025$  and apply the laser stirrer for  $\tau = 40$  ms. It is rotating with  $\Omega'$  either with the same (excitation of  $m = +2$ ) or the opposite sense ( $m = -2$ ) with respect to the vortex. We perform the usual time of flight and imaging and measure the ellipticity  $\zeta$  as a function of  $\Omega'$ . We observe a clear resonance for each mode (Fig. 2). The two resonances occur at different central frequencies according to the already mentioned lift of degeneracy. The key feature of the present study is that the width of the  $m = -2$  resonance is significantly larger than that of  $m = +2$ . Hence, as seen before, the vortex causes larger damping for the counterrotating surface wave than for the corotating.

To analyze our data, we assume that the amplitude of the relevant mode varies according to Eq. (2) with a driving term  $Ae^{-2i\Omega't}$  on the right-hand side. This assumption leads to a good fit to the data (Fig. 2) and yields  $\omega_{+2}/2\pi = 161.0 \pm 1.0$  Hz,  $\omega_{-2}/2\pi = 119.8 \pm 1.0$  Hz.

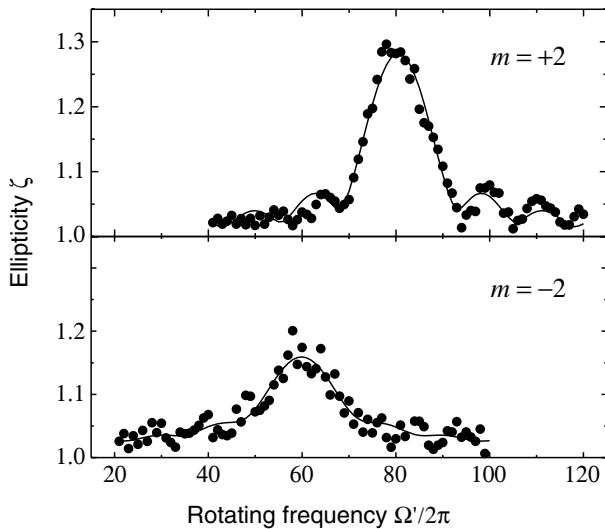


FIG. 2. Resonance of the ellipticity  $\zeta$  for the  $m = +2$  and  $m = -2$  modes. The lines are fits deduced from the solution of Eq. (2) with a sinusoidal drive. The resonance of the mode  $m = -2$  is broader than that of the  $m = +2$ , as a consequence of a larger damping rate.

These frequencies are in excellent agreement with those obtained by the percussional excitation. The  $\sim 2$  Hz shift is due to the increase of the trapping frequency by the laser stirrer. The fitted damping rates are  $\Gamma_{+2} = 24 \pm 5 \text{ s}^{-1}$  and  $\Gamma_{-2} = 57 \pm 10 \text{ s}^{-1}$ . These are slightly larger than those obtained from the percussional experiment, possibly due to an additional heating caused by the stirrer. However, the main feature  $\Gamma_{-2} \sim 2\Gamma_{+2}$  remains valid.

We now discuss the possible physical origin of this increased damping of the  $m = -2$  mode. The starting point of our analysis is the behavior of the uncondensed part of the gas. Is it still rotating when we perform the percussional or near resonant excitation? If it rotates, the symmetry between the two senses of rotation is broken and the corotating mode experiences less friction than the counterrotating mode. In [30], it has been shown that in this case  $\Gamma_{-2} > \Gamma_{+2}^{(0)}$  and  $\Gamma_{+2} < \Gamma_{-2}^{(0)}$ . Moreover, one gets  $\Gamma_{-2} + \Gamma_{+2} \approx 2\Gamma_{\pm 2}^{(0)}$ . This latter relation does not correspond to our observations. Although we do observe an increase of  $\Gamma_{-2}$  when a vortex has been nucleated, we do not observe a corresponding reduction of  $\Gamma_{+2}$ . From this we infer that the uncondensed fraction does not rotate significantly in our experiment. Furthermore, no such rotation is expected for our experimental conditions. The  $\sim 1\%$  static trap anisotropy, which barely affects the behavior of the condensate, rapidly damps the rotation of a noncondensed gas [31,32]. The thermal cloud thus experiences two competitive forces in the bare magnetic trap: a rotational drive from the velocity flow of the condensate and a friction from the static trap anisotropy. Unlike in the case of a complete vortex array [33], the rotational drive due to a condensate with a single vortex is

small compared to the friction term. Therefore the rotation of the thermal cloud is expected to be negligible.

Assuming now that the uncondensed gas is at rest, the other possible reason for a faster damping of the  $m = -2$  mode is the existence of a decay channel open for  $m = -2$  and closed for  $m = +2$ . The natural candidate for this mechanism is the Beliaev conversion of the  $m = -2$  mode into two Kelvin modes  $k$  and  $-k$  [34]. Since the Kelvin excitations have negative angular momentum with respect to the vortex charge, this mechanism is specific to the  $m = -2$  mode. A recent theoretical analysis of this decay process, taking into account both Beliaev and Landau damping, has led to damping rates in good agreement with those that we measure experimentally [35].

To support this interpretation, we present time-of-flight images of the vortex line. The images are taken immediately after the excitation of the  $m = -2$  or  $m = +2$  mode. For each mode we choose  $\Omega'$  at the center of the resonance and apply the probe for  $\tau = 33 \text{ ms}$ . Figure 3 shows two condensates in the transverse view. The left picture [Fig. 3(a)] was taken counterrotating ( $m = -2$ ), the right picture [Fig. 3(b)] corotating ( $m = +2$ ). Below these are shown the horizontal density profiles taken at the center of the vortex line [Figs. 3(c) and 3(d)].

The vortex line is visible in both images with good contrast. As already observed in [20], the line at equilibrium is curved at both ends. It takes in the present case the form of an unfolded “N” (similar results have been obtained with “U shaped” lines). After excitation of the  $m = -2$  mode, the atom density presents a periodic structure apparent as vertical stripes in the vicinity of the vortex line [Figs. 3(a) and 3(c)]. A Fourier analysis of the density profile reveals a peak centered at  $k_0 = 0.70 \mu\text{m}^{-1}$  with a full width at half maximum  $\Delta k_0 \approx 0.15 \mu\text{m}^{-1}$ . The area of the peak, which can be observed reproducibly

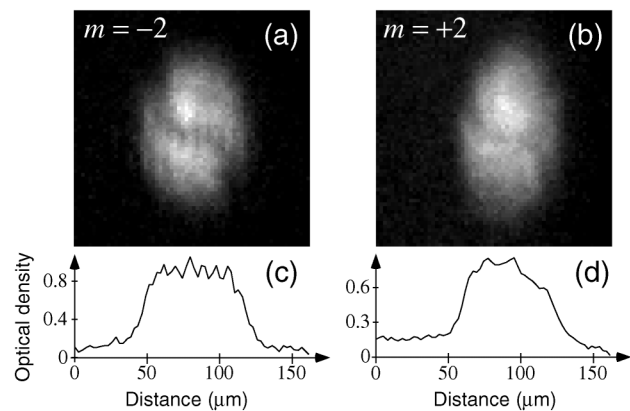


FIG. 3. Transverse images of the condensate after a 33 ms resonant excitation of the  $m = -2$  mode (a) and the  $m = +2$  mode (b). The picture on the left shows a periodic structure superimposed on the vortex line. The horizontal density profiles (c),(d) have been obtained by averaging over three vertical pixels around the center of the vortex line.

for similar experimental conditions, is 6 standard deviations above noise. On the contrary, such a periodic structure never appears in the images corresponding to  $m = +2$  [see, e.g., Figs. 3(b) and 3(d)].

This observation supports the proposed decay mechanism of the  $m = -2$  mode into a pair of Kelvin modes. At any given time, the excited vortex line is expected to have an almost sinusoidal shape with a spatial period of  $2\pi/k$  along the  $z$  axis. It is located in a plane containing the  $z$  axis and rotating around this axis in the sense opposite to the vortex. At the center of the condensate, the healing length is  $\xi \sim 0.3 \mu\text{m}$ . Using Eq. (1) and energy conservation, we find  $k = 0.8 \mu\text{m}^{-1}$ . Assuming that during the time of flight, the expansion factor  $\Lambda_z$  along the  $z$  axis is the same for the shape of the vortex line as it is for the longitudinal size of the condensate ( $\Lambda_z \sim 1.3$  [36]), we recover the measured wave vector  $k_0$  within  $\Delta k_0$ . This gives approximately nine oscillation periods over the  $L \sim 70 \mu\text{m}$  length of the condensate, which is consistent with the observation in Fig. 3(a). With the quantization condition  $k = \mathcal{N}\pi/L$  for the vortex line, we get  $\mathcal{N} \sim 18$ . The splitting between the adjacent Kelvin modes is then  $\sim 20 \text{ s}^{-1}$ , so that we have one or two Kelvin modes within the width  $\Gamma_{\pm 2}^{(0)}$  of the quadrupole resonance. We note that a detailed treatment of the relation between the observed density modulation and the oscillations of the vortex line remains to be done. The principle of such a treatment may follow that of Ref. [37], where phase fluctuations due to a short coherence length in a quasi-condensate appear as density fluctuations after a time of flight.

In conclusion, we have observed a strong difference between the damping rates of the corotating ( $m = +2$ ) and counterrotating ( $m = -2$ ) quadrupole modes of a single vortex condensate. We explain this difference as due to the decay of the  $m = -2$  mode into Kelvin excitations of the vortex line. This is confirmed by images of the condensate, which show a spatial density modulation around the vortex line only for counterrotating excitation.

We thank K. Madison for participation in earlier stages of this experiment, and L. Carr, Y. Castin, and K. Machida for useful discussions. P.R. acknowledges support by the Alexander-von-Humboldt Stiftung and the EU (Contract No. HPMF CT 2000 00830). This work is partially supported by CNRS, Collège de France, Région Ile de France, DGA, DRED, and EU (Contract No. HPRN-CT-2000-00125).

\*Also at FOM Institute for Atomic and Molecular Physics, Amsterdam, The Netherlands, and Russian Research Center Kurchatov Institute, Moscow, Russia.

†Unité de Recherche de l'École normale supérieure et de l'Université Pierre et Marie Curie, associée au CNRS.

[1] L. Onsager, *Nuovo Cimento* **6**, Suppl. 2, 249 (1949).

- [2] R. P. Feynman, in *Progress in Low Temperature Physics*, edited by C. J. Gorter (North-Holland, Amsterdam, 1955), Vol. 1, Chap. 2.
- [3] E. M. Lifshitz and L. P. Pitaevskii, *Statistical Physics, Pt. 2* (Butterworth-Heinemann, Oxford, 1980), Chap. III.
- [4] M. Tinkham, *Introduction to Superconductivity* (McGraw-Hill, New York, 1996).
- [5] R. J. Donnelly, *Quantized Vortices in Helium II* (Cambridge University Press, Cambridge, 1991).
- [6] M. R. Matthews *et al.*, *Phys. Rev. Lett.* **83**, 2498 (1999).
- [7] K. W. Madison *et al.*, *Phys. Rev. Lett.* **84**, 806 (2000).
- [8] J. R. Abo-Shaeer *et al.*, *Science* **292**, 476 (2001); C. Raman *et al.*, *Phys. Rev. Lett.* **87**, 210402 (2001).
- [9] E. Hodby *et al.*, *Phys. Rev. Lett.* **86**, 2196 (2001).
- [10] W. Thomson (Lord Kelvin), *Philos. Mag.* **10**, 155 (1880).
- [11] L. P. Pitaevskii, *Sov. Phys. JETP* **13**, 451 (1961).
- [12] A. L. Fetter, *Phys. Rev.* **162**, 143 (1967).
- [13] L. D. Landau and E. M. Lifshitz, *Fluid Mechanics* (Pergamon Press, London, 1987), Sec. 8.
- [14] R. I. Epstein and G. Baym, *Astrophys. J.* **387**, 276 (1992).
- [15] E. B. Sonin, *Rev. Mod. Phys.* **59**, 87 (1987).
- [16] R. A. Ashton and W. I. Glaberson, *Phys. Rev. Lett.* **42**, 1062 (1979).
- [17] T. Isoshima and K. Machida, *Phys. Rev. A* **59**, 2203 (1999).
- [18] A. A. Svidzinsky and A. L. Fetter, *Phys. Rev. A* **62**, 063617 (2000).
- [19] When several vortices are present and interact together, the nature of the excitations changes and Tkachenko modes appear (see, e.g., [15]). The quadrupole modes under study can then couple to these collective lattice modes as observed in P. Engels *et al.*, *Phys. Rev. Lett.* **89**, 100403 (2002).
- [20] P. Rosenbusch, V. Bretin, and J. Dalibard, *Phys. Rev. Lett.* **89**, 200403 (2002).
- [21] R. Dodd *et al.*, *Phys. Rev. A* **56**, 587 (1997).
- [22] S. Sinha, *Phys. Rev. A* **55**, 4325 (1997).
- [23] A. A. Svidzinsky and A. L. Fetter, *Phys. Rev. A* **58**, 3168 (1998).
- [24] F. Zambelli and S. Stringari, *Phys. Rev. Lett.* **81**, 1754 (1998).
- [25] F. Chevy, K. W. Madison, and J. Dalibard, *Phys. Rev. Lett.* **85**, 2223 (2000).
- [26] P. C. Haljan *et al.*, *Phys. Rev. Lett.* **86**, 2922 (2001).
- [27] A. E. Leanhardt *et al.*, cond-mat/0206303.
- [28] S. Stringari, *Phys. Rev. Lett.* **77**, 2360 (1996).
- [29] Without the constraint of symmetry between the modes  $m = \pm 2$ , the zero-vortex data lead to  $\omega_{+2}^{(0)}/2\pi = 142.4 \text{ Hz}$ ,  $\omega_{-2}^{(0)}/2\pi = 141.2 \text{ Hz}$ ,  $\Gamma_{+2}^{(0)} = 22.6 \text{ s}^{-1}$ ,  $\Gamma_{-2}^{(0)} = 20.0 \text{ s}^{-1}$ .
- [30] J. E. Williams *et al.*, *Phys. Rev. Lett.* **88**, 070401 (2002).
- [31] D. Guéry-Odelin, *Phys. Rev. A* **62**, 033607 (2000).
- [32] P. C. Haljan *et al.*, *Phys. Rev. Lett.* **87**, 210403 (2001).
- [33] O. N. Zhuravlev, A. E. Muryshev, and P. O. Fedichev, *Phys. Rev. A* **64**, 053601 (2001).
- [34] Each kelvon can subsequently decay into another kelvon with a slightly smaller momentum and a phonon.
- [35] T. Mizushima *et al.*, cond-mat/0211396.
- [36] Y. Castin and R. Dum, *Phys. Rev. Lett.* **77**, 5315 (1996).
- [37] S. Dettmer *et al.*, *Phys. Rev. Lett.* **87**, 160406 (2001).